

Cosmic Ray composition around the knee from EAS electromagnetic and muon data

G. Navarra for the EAS-TOP and MACRO Collaboration

Dipartimento di Fisica Generale dell'Università di Torino and INFN, Italy

Abstract. We present the results of the studies of the cosmic ray primary composition around the knee of the spectrum performed by EAS-TOP (2005 m a.s.l., 10^5 m² collecting area) and MACRO (963 m a.s.l., 3100 m w.e. of minimum rock overburden, 920 m² effective area) at the National Gran Sasso Laboratories. The used observables are the shower size (N_e) measured by EAS-TOP and the muon number (N_μ) recorded by MACRO. The results support a primary composition becoming heavier at the knee of the primary spectrum. The observables used in the analysis are the results of secondary particles produced in the early stages of the shower development and in kinematic region quite different from the one relevant for the usual $N_\mu - N_e$ studies.

1 Introduction

The study of the primary composition in the Extensive Air Shower energy region requires the use of different observables in order to cross check the information and reduce the dependence on the interaction model and propagation codes used. At the National Gran Sasso Laboratories a program of exploiting the surface shower size measurements from EAS-TOP (2005 m a.s.l.), and the high energy muon measurements ($E_\mu^{th} = 1.3$ TeV) performed in the deep underground laboratories (MACRO) has been developed. Such muons in fact originate from the decays of mesons produced in the first interactions in the atmosphere and from a quite different rapidity region than the GeV muons usually used for such analysis ($x_F > 0.1$ or 0.2).

The two experiments operated in coincidence for a live time of $\Delta T = 960.12$ days between 1990 and 2000. The number of coincident events collected with the two detectors operating in the final configuration amounts to 28160, of which 3752 have shower cores inside the edges of the array ("internal events") and shower size $N_e > 2 \cdot 10^5$, and 409 have $N_e > 10^{5.92}$, i.e. above the observed knee at the

corresponding zenith angle. We present here a first analysis of the full data set, by using full simulations of the detectors (based on GEANT), and of the cascades in the atmosphere performed inside the same frame as for the surface data (CORSIKA). Further details and partial results of the present work can be found in R. Bellotti et al, 1990 and EAS-TOP/MACRO Coll., 1994.

2 The detectors

The EAS-TOP array is located at Campo Imperatore (2005 m a.s.l., $\approx 30^\circ$ with respect to the vertical of the underground Gran Sasso Laboratories, corresponding to 930 gr cm⁻² atmospheric depth). Its e.m. detector (to which we are mainly interested in the present analysis) is built of 35 scintillator modules 10 m² each, including an area $A \approx 10^5$ m². The array is fully efficient for $N_e > 10^5$. Its reconstruction capabilities of the EAS parameters (for internal events) are: $\frac{\Delta N_e}{N_e} \approx 10\%$ above $N_e \approx 10^5$, and $\Delta\theta \approx 0.9^\circ$ for the EAS arrival direction. The array and the reconstruction procedures are fully described in M. Aglietta et al, 1993.

MACRO, in the underground Gran Sasso Laboratory at 963 m a.s.l., with 3100 m w.e. of minimum rock overburden, is a large area multi-purpose apparatus designed to detect penetrating cosmic radiation. The lower part of the MACRO detector has dimensions $76.6 \times 12 \times 4.8$ m³. A detailed description of the apparatus can be found in MACRO Collaboration, 1993. In this work we consider only muon tracks which have at least 4 aligned hits in both views of the horizontal streamer tube planes over the 10 layers composing the whole detector. The standard reconstruction procedure of MACRO (MACRO Collaboration, 1992) has been used, which provides an accuracy due to the instrumental uncertainties and the muon scattering in the rock of 0.95° for the muon arrival direction. The muon number is measured with accuracy $\Delta N_\mu=1$; high multiplicity events have been scanned by eye to avoid possible misinterpretations. ($\Delta N_\mu=2$ will be the multiplicity bin used in the analysis, independent of the

track density of the event.) The two experiments are separated by a thickness of rock ranging from 1100 up to 1300 m, depending on the angle. The muon energy threshold at the surface for muons reaching the MACRO depth ranges from $E_\mu^{th} = 1.3$ TeV to $E_\mu^{th} = 1.8$ TeV inside the effective area of EAS-TOP. Event coincidence is established off-line, using the absolute time given by a GPS system with an accuracy better than $1 \mu s$.

Independent analyses of the two arrays are in MACRO Coll., 1997, and EAS-TOP Coll., 1999. Simulations are performed for the four interaction models included in the CORSIKA package (Knapp and Heck, 1998), the MUSIC code (P. Antonioli et al., 1997) for the muon transport in the rock, and the GEANT code for detector simulations.

3 Analysis and results

The analysis technique has to be adapted to the specific trigger requirements (both surface and underground detectors fired) with defined acceptance area for the EAS array (internal events), but undefined for the underground one. Therefore, the main experimental feature to be considered is the muon multiplicity distribution in different intervals of shower sizes. We have chosen four intervals of shower sizes around the knee:

$5.31 < \text{Log}_{10}(Ne) \leq 5.61$; $5.61 < \text{Log}_{10}(Ne) \leq 5.92$; $5.92 < \text{Log}_{10}(Ne) \leq 6.15$; and $\text{Log}_{10}(Ne) > 6.15$

The assumptions made for the present analysis are the following.

- Within each size bin, the fraction of each mass component contributing to that size bin is practically constant in energy. (This is not straightforward since, for a given mass, the energies contributing to the same size interval differ of a factor up to 2.) All spectra in the simulation have slope $\gamma = 2.62$.

- Each multiplicity distribution can be reproduced by a linear combination of simulated distributions obtained from individual components.

- Concerning the number of independent mass components to be considered in the fit, we verified with the simulated data that the multiplicity distribution (in a given size bin) due to a mass component which is intermediate between the two extremes (p and Fe) can be reproduced by a proper combination of these extremes. As a cross-check, we have tried to fit the multiplicity distribution as a sum of more than two contributions from different mass components; in each attempt the minimization program acts so to give null weight to the intermediate masses. This demonstrates that (inside the sensitivity of the measurement) the distributions can be already accounted for in the combination of the extremes. Therefore the experimental data have been fitted using just the proton and Fe contributions.

The fit has been performed in the quoted four windows by minimizing the following function for each multiplicity

distribution:

$$\chi^2 = \sum_i \frac{(N_i^{exp} - p_1 N_i^p - p_2 N_i^{Fe})^2}{\sigma_{i,exp}^2} \quad (1)$$

where N_i^{exp} is the number of observed events in the i -th bin of multiplicity, N^p and N^{Fe} are the number of simulated events in the same i -th multiplicity bin from the p and Fe components, respectively; p_1 and p_2 are the parameters (to be fitted) defining the fraction of each mass component contributing to the same multiplicity bin, and only multiplicities up to 20 have been used. The fit results have been normalized to reproduce the observed number of coincident events in each size bin. In this way we have obtained the abundances of protons and iron nuclei as a function of the size and, as a consequence, the obtained size spectrum is by construction in agreement with the experimental one, for the same binning. In Fig. 1 we show, as examples, the multiplicity distributions in the second and third size bins, together with the p and Fe simulations, for QGSJET, and the fit results. The exchange in the predominance of p and Fe primaries going through the knee is clearly seen from the changing tail of the multiplicity distribution. The value of the coefficients for the two components and all the four interaction models are reported in Tab. 1, and all of them show a tendency towards an heavier composition through the size of the knee.

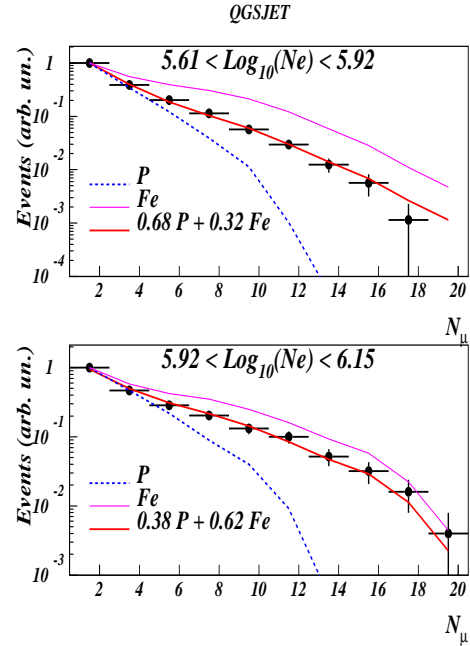


Fig. 1. Example of experimental multiplicity distributions in two size bins across the knee observed in the e.m. size, together with the results of the fits for the QGSJET interaction model.

In Fig. 2 we present $N_e^{2.5}$ times the size spectrum, for coincident events, as compared with one of the simulation sets. The agreement is good, showing that the procedure used, and particularly the bin size, is appropriate for this analysis. This figure also shows that, within the limited statistics, the knee

	QGSJET	HDPM	DPMJET	Sibyll
$5.31 < \text{Log}_{10}(N_e) < 5.61$; 2352 events				
p	0.66 ± 0.04	0.45 ± 0.04	0.65 ± 0.04	0.49 ± 0.04
Fe	0.34 ± 0.03	0.55 ± 0.03	0.35 ± 0.03	0.51 ± 0.03
$5.61 < \text{Log}_{10}(N_e) < 5.92$; 881 events				
p	0.68 ± 0.05	0.45 ± 0.05	0.67 ± 0.05	0.48 ± 0.06
Fe	0.32 ± 0.04	0.55 ± 0.07	0.33 ± 0.04	0.52 ± 0.05
$5.92 < \text{Log}_{10}(N_e) < 6.15$; 252 events				
p	0.38 ± 0.10	0.36 ± 0.09	0.45 ± 0.09	0.30 ± 0.09
Fe	0.62 ± 0.09	0.64 ± 0.07	0.55 ± 0.10	0.70 ± 0.08
$\text{Log}_{10}(N_e) > 6.15$; 157 events				
p	0.30 ± 0.15	0.04 ± 0.12	0.44 ± 0.13	0.37 ± 0.12
Fe	0.70 ± 0.26	0.96 ± 0.18	0.54 ± 0.16	0.63 ± 0.15

Table 1. Coefficients of the two components used in the fit (after normalization), in the four bins in N_e . The errors on these coefficients are not independent (almost full anti-correlation)

in the size distribution is evident and well reproduced by the simulation.

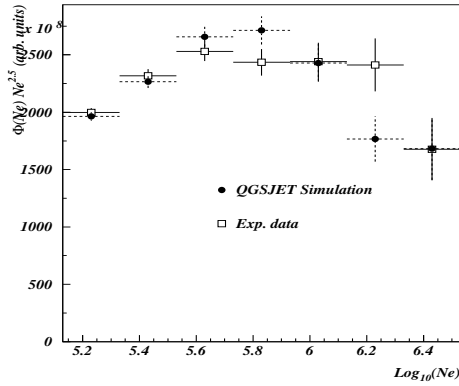


Fig. 2. Size spectrum for coincident events: data and Monte Carlo (QGSJET) reconstruction (after fit) are shown

The values of parameters p_1 and p_2 resulting from the fit cannot be immediately translated into a physically meaningful composition, since we started from simulated distributions which already included triggering efficiency. (No trigger is generated for events with $N_\mu = 0$.) We have to take into account that for primary energies corresponding to size values exceeding 10^5 , heavy primaries (*i.e.* those who originate in the average larger multiplicity events over a wider area) have a higher probability to trigger the underground detector. The relative correction in triggering probability between the two mass components can be obtained as a function of $\text{Log}(E)$ from the simulation in the form of a table of coefficients w_k which must be used to assign a relative weight to the two extreme components. In the framework of a 2-component fit, we define w_k as the relative weight of Fe nuclei to proton primaries in the k -th bin of $\text{Log}(E)$.

To infer the mass composition evolution as a function of energy, for each size bin we take from the simulation the $\text{Log}(E)$ distributions of contributing p and Fe weighted by

the parameters p_1 and p_2 and with the relative weight w_k . The resulting distributions from different size bins are summed together, and so we eventually obtain the simulated energy spectra of the two basic components that reproduce the experimental data. These resulting spectra for p and Fe (re-

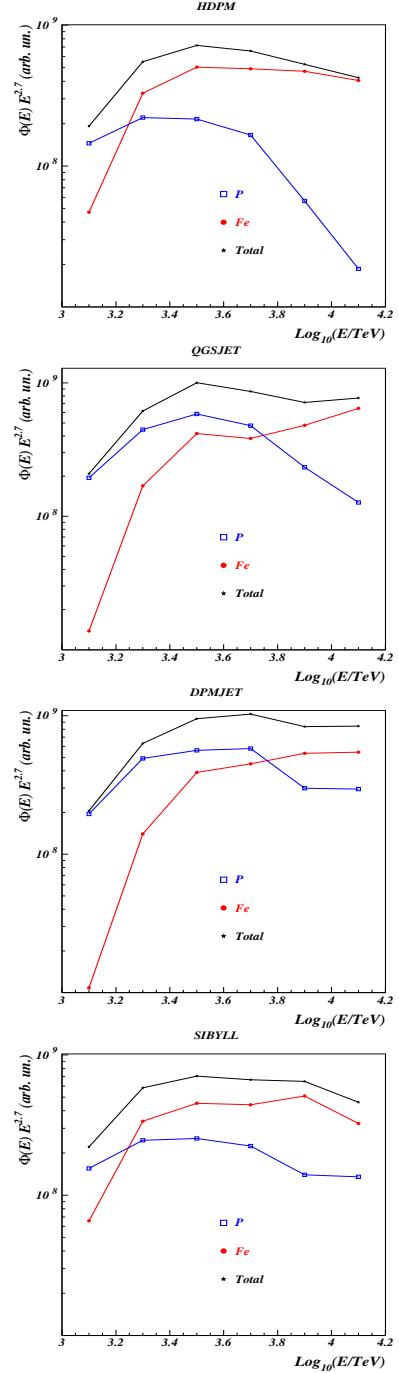


Fig. 3. Energy spectra for p (a) and Fe (b) components, and their sum, as resulting from the analysis for the different interaction models.

ported in Fig. 3) should not be interpreted as a measurement of the real p and Fe fluxes, but as a sort of effective ‘‘Light’’

and ‘‘Heavy’’ components, each one of them representing the overall average behavior of different individual mass components. Then, for each bin in $\text{Log}(E)$ we calculate $\langle \log A \rangle$ from the expression:

$$\langle \log A \rangle = \frac{p_1 M_k^p \text{Log}(A^p) + p_2 w_k M_k^{Fe} \text{Log}(A^{Fe})}{M_k^p + p_2 w_k M_k^{Fe}} \quad (2)$$

where M_k^p and M_k^{Fe} are the numbers of simulated events from p and Fe contributing at the k-th energy bin. The results are depicted in Fig. 4 for each interaction model, the two curves delimiting the error band. The results for all interaction models show an increase in $\langle \log A \rangle$ through the energy corresponding to the knee position. This is less evident for this version of Sibyll. This model, together with HDPM, seems to lead to a composition quite heavier than those suggested from QGSJET and DPMJET, just above 10^{15} eV. An analysis of the interaction models excluding the possibility of using Sibyll in this energy range has been performed, through the hadron data, by KASCADE (Hörandel J., 1999).

4 Conclusions

The first analysis of the full statistics of the internal N_e - N_μ^{TeV} events collected by the MACRO/EAS-TOP Collaboration in about 10 years of data taking at the Gran Sasso Laboratories points to a primary composition becoming heavier around the knee of the primary spectrum (in the energy region 10^{15} – 10^{16} eV). Quantitative conclusions depend on the theoretical uncertainties of the hadronic interaction models. The most theoretically founded models (QGSJET, DPMJET) provide, at the lower energies ($\approx 10^{15}$ eV), results which are near to the extrapolations of the low energy data. However, the study of all systematic uncertainties in the analysis method has not yet been completed.

References

- Aglietta M. et al., Nucl. Instr. & Meth. A, 336, 310, 1993.
 Antonioli P. et al., Astrop. Physics 7, 357, 1997.
 Bellotti R. et al, 1990, Phys. Rev D, 42, 1396.
 EAS-TOP Coll., Astroparticle Physics, 10, 1, 1999, and Proc. 26th ICRC, 1, 230, 1999.
 EAS-TOP and MACRO Coll., 1994, Phys. Lett. B, 337, 376.
 Hörandel J. et al, J. Phys. G, 24, 2161, 1999.
 MACRO Collaboration (Ahlen S.P. et al.), Nucl. Instr. & Meth. A, 324, 337, 1993.
 MACRO Collaboration (Ahlen S.P. et al.), Phys. Rev. D, 46, 4836, 1992.
 Knapp J. and Heck D., Extensive Air Shower Simulation with CORSIKA (Version 5.61), 1998.
 MACRO Collaboration (Ambrosio M. et al.), Phys. Rev. D, 56, 1418, 1997.

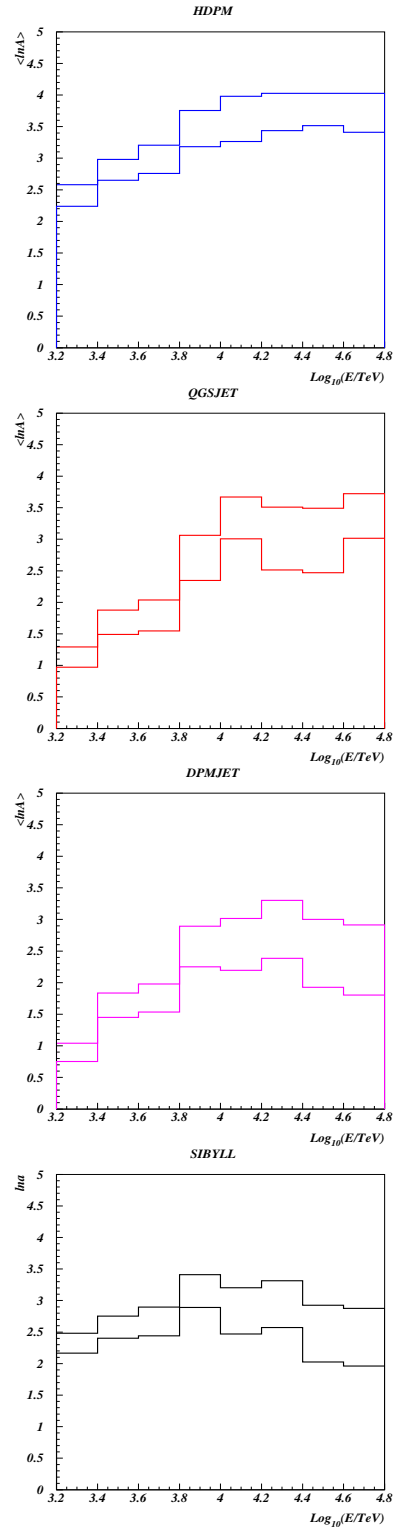


Fig. 4. $\langle \log A \rangle$ vs energy as resulting from different interaction models. The two lines include the statistical error.